

Anisotropic optical conductivity of the putative Kondo insulator CeRu₄Sn₆V. Guritanu,¹ P. Wissgott,² T. Weig,³ H. Winkler,² J. Sichelschmidt,¹ M. Scheffler,³ A. Prokofiev,² S. Kimura,⁴ T. Iizuka,⁴ A. M. Strydom,⁵ M. Dressel,³ F. Steglich,¹ K. Held,² and S. Paschen²¹Max Planck Institute for Chemical Physics of Solids, 01187 Dresden, Germany²Institute of Solid State Physics, Vienna University of Technology, Wiedner Hauptstrasse 8-10, 1040 Vienna, Austria³I. Physikalisches Institut, Universität Stuttgart, 70550 Stuttgart, Germany⁴UVSOR Facility, Institute for Molecular Science, Okazaki 444-8585, Japan⁵Physics Department, University of Johannesburg, Auckland Park 2006, South Africa

(Received 13 September 2012; published 21 March 2013)

Kondo insulators and in particular their noncubic representatives have remained poorly understood. Here we report on the development of an anisotropic energy pseudogap in the tetragonal compound CeRu₄Sn₆ employing optical reflectivity measurements in broad frequency and temperature ranges. The low-energy optical conductivity shows semiconductor-like features within the *a*-*a* plane but a Drude-like response along the *c* axis, signaling weak metallicity. Local density approximation plus dynamical mean-field theory calculations reproduce these observations qualitatively and help to identify their origin. For large parts of the Brillouin zone, the strongly correlated band structure presents a narrow direct gap within the Kondo resonance. Only for the *c* direction, due to anisotropy in the hybridization, there is a pronounced band crossing at the Fermi level.

DOI: [10.1103/PhysRevB.87.115129](https://doi.org/10.1103/PhysRevB.87.115129)

PACS number(s): 71.27.+a, 71.15.Mb, 78.20.-e

Correlated materials with gapped or pseudogapped ground states continue to be of great interest. The gap in the electronic density of states (DOS) either opens gradually with decreasing temperature, as is the case for the pseudogap of high-temperature superconductors,¹ or emerges at a continuous or first-order phase transition.²⁻⁴ In heavy fermion compounds⁵—systems in which *f* and conduction electrons strongly interact—a narrow hybridization gap is known to emerge gradually.⁶⁻⁹ Generically, the Fermi energy is situated in one of the hybridized bands and a metallic heavy-fermion ground state arises. Only for special cases does the Fermi energy lie within the gap and the ground state is Kondo insulating. Metallic heavy-fermion systems have been intensively investigated over the past decades and are now, at least away from quantum criticality,¹⁰ well understood¹¹ within the framework of Landau Fermi liquid theory. Hence, few parameters, most notably the effective mass, allow us to describe thermodynamic and transport properties at the lowest temperatures. In comparison, the physics of Kondo insulators has proven to be much less tractable. This is due at least in part to the fact that the gapped ground state inhibits a characterization via the above properties. Many experimental efforts have therefore focused on the determination of the gap width from temperature dependencies, which has frequently led to conflicting results, in particular for anisotropic Kondo insulators such as CeNiSn.¹² Here the strongly anisotropic transport and magnetic properties have been interpreted phenomenologically on the basis of a V-shaped DOS (Ref. 13) or by invoking a hybridization gap with nodes¹⁴⁻¹⁶ or extrinsic effects such as impurities, off-stoichiometry, or strain.^{17,18} To advance the field, it appears to be mandatory to model a number of carefully chosen materials *ab initio*, taking all essential ingredients into account.

Here we investigate CeRu₄Sn₆, which due to its tetragonal crystal structure is simpler than the previously studied orthorhombic materials. In a combined experimental and theoretical effort, we provide direct spectroscopic evidence

for the development of an anisotropic pseudogap: While weak metallicity prevails in the optical conductivity along the *c* axis, insulator-like behavior without a Drude peak is observed in the *a*-*a* plane. We trace this back to a correlated band structure which is essentially gapped, except for the *c* direction, as shown by the local density approximation (LDA) plus dynamical mean-field theory (DMFT) calculations.

CeRu₄Sn₆ crystallizes in the tetragonal *I* $\bar{4}$ 2*m* structure,^{19,20} with *a* = 6.8810 Å and *c* = 9.7520 Å. Single crystals were grown from self-flux, using the floating zone melting technique with optical heating.²¹ Near-normal incidence reflectivity spectra on the *ac* plane were measured using linearly polarized light, with the electric field *E* ∥ *a* and *E* ∥ *c*, in a broad energy range from 0.5 meV to 30 eV with the following techniques: a coherent-source spectrometer in the terahertz (THz) energy range (0.5–5 meV),²² a Fourier transform spectrometer (Bruker IFS 66 v/S) with a reference gold layer evaporated in situ on the sample surface for 5 meV–0.68 eV, a JASCO FTIR 610 spectrometer with an Al mirror as reference for 0.6–1.25 eV, and synchrotron radiation for 1.2–30 eV (beamline 7B of UVSOR-II). Between 5 meV and 0.68 eV, a magnetic field of 7 T applied to polycrystalline CeRu₄Sn₆ did not change the reflectivity appreciably.

The theoretical optical conductivity was derived from DMFT combined with the LDA within density functional theory.^{23,24} We performed a full-potential WIEN2K (Ref. 25) LDA calculation with spin-orbit coupling, and projected the Bloch waves onto maximally localized Wannier orbitals of Ce-4*f*, Ru-4*d*, and Sn-5*p* character.^{26,27} For this basis and a typical Coulomb repulsion of *U* = 5.5 eV for Ce,²⁸ we included electronic correlations by DMFT using quantum Monte Carlo simulations²⁹ for the *J* = 5/2 subset of the Ce 4*f* orbitals around the Fermi energy. The optical conductivity was calculated as described in Ref. 30, with an additional imaginary part of the self-energy of 50 meV to account for impurity scattering and a minor readjustment of the chemical potential by 50 meV due to different *k* meshes employed.

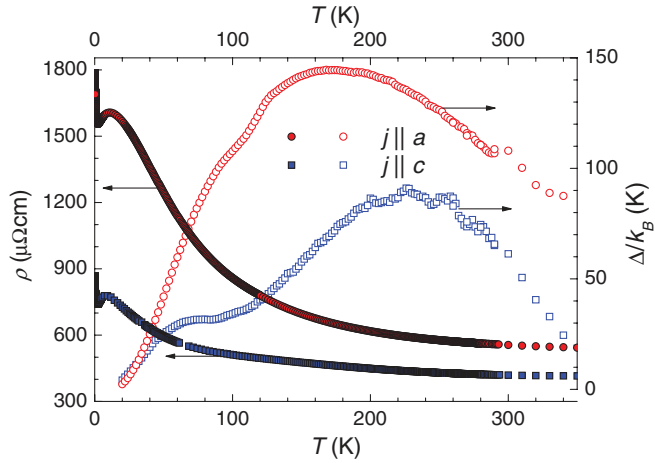


FIG. 1. (Color online) Temperature-dependent electrical resistivity, $\rho(T)$ (left), and fitted energy gap in units of temperature, Δ/k_B (right, see text), for single-crystalline CeRu_4Sn_6 , with the current density j along the a and c axes. c' axis (diagonal of a - a plane) data were previously published.²¹

As mentioned above, attempts to characterize Kondo insulators by a single, temperature-independent energy gap have generally failed. This is also the case for CeRu_4Sn_6 , as illustrated by temperature-dependent electrical resistivity, $\rho(T)$, data along the two principal axes a and c (Fig. 1, left axis). As for other noncubic systems [e.g., CeNiSn ,³¹ $\text{U}_2\text{Ru}_2\text{Sn}$,³² and $\text{CeFe}_2\text{Al}_{10}$ (Ref. 33)], a pronounced anisotropy is observed. The temperature-dependent energy gaps $\Delta(T)$ for the two directions (Fig. 1, right axis) were obtained by fitting the $\rho(T)$ data in 20 K ranges with an Arrhenius law $\rho = \rho_0 \exp[\Delta/(2k_B T)]$. Our results confirm that the definition of a unique energy gap scale characterizing the material seems

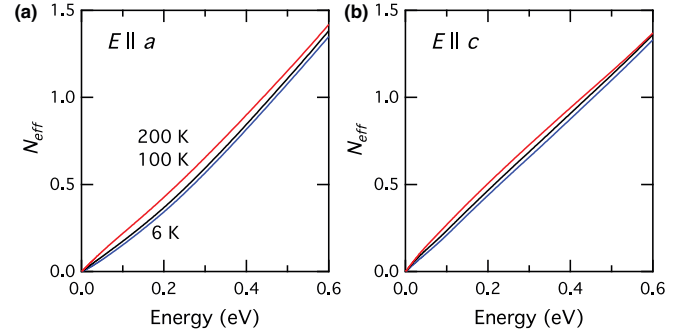


FIG. 3. (Color online) Integrated spectral weight of single-crystalline CeRu_4Sn_6 at 6, 100, and 200 K for $E \parallel a$ (a) and $E \parallel c$ (b).

arbitrary. Modeling temperature-dependent data with fine-structured (V-shaped or more complex) free-electron bands yields improved fits³⁴ but provides little new insight. This clearly calls for a rethinking of the problem and a different approach, which is what we present here.

Optical spectroscopy is a powerful tool to characterize strongly correlated materials since the low-energy scales in these systems can be ideally probed by optical excitations in the far-infrared and THz frequency range. The optical reflectivity spectra, $R(\omega)$, of CeRu_4Sn_6 develop a sizable temperature dependence at low energies [Figs. 2(a) and 2(b)]. This effect is larger for the a axis, in agreement with the steeper increase of the a axis $\rho(T)$ with decreasing temperature (Fig. 1).

The frequency-dependent real part of the optical conductivity, $\sigma_1(\omega)$, was derived from the reflectivity data using a Kramers-Kronig fitting procedure.^{35,36} $\sigma_1(\omega)$ shows pronounced a - c anisotropy [Figs. 2(c)–2(f)], in particular at low temperatures: While the continuous decrease of $\sigma_1(\omega)$ with decreasing energy observed for the a axis is a feature of

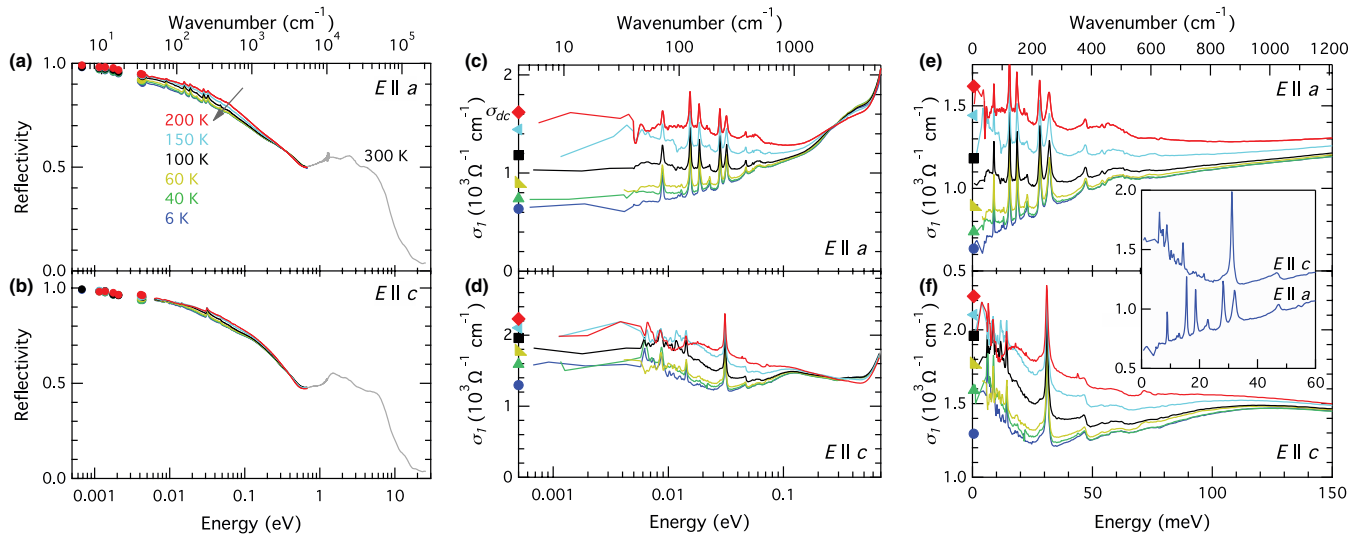


FIG. 2. (Color online) (a,b) Normal-incidence reflectivity spectra of single-crystalline CeRu_4Sn_6 at various temperatures for $E \parallel a$ and $E \parallel c$, respectively. (c,d) Real parts of the optical conductivity, $\sigma_1(\omega)$, for $E \parallel a$ and $E \parallel c$, respectively. The filled circles on the vertical axis represent the independently measured dc conductivity data at the corresponding temperatures. (e,f) Low-energy part of $\sigma_1(\omega)$, with the inset showing semiconductor-like behavior and weak metallicity for $E \parallel a$ and $E \parallel c$, respectively. The sharp features in (c-f) (at 8.9, 15.5, 18.6, 28, and 31.6 meV along the a axis, and at 8.7, 14.4, and 30.9 meV along the c axis) are phonon modes. They are temperature-independent within our resolution ($2 \text{ cm}^{-1} \equiv 0.25 \text{ meV}$).

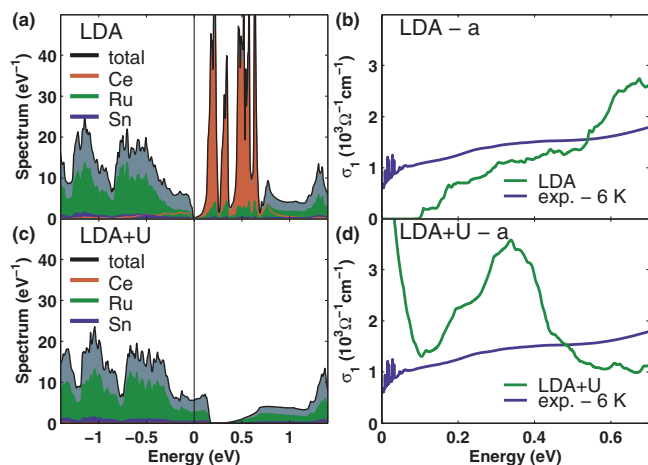


FIG. 4. (Color online) DOS and corresponding a axis $\sigma_1(\omega)$ obtained by LDA (a,b) and LDA + U (c,d). The calculated c -axis conductivities are similar (not shown).

semiconductors, the upturn seen below 30 meV for the c axis signals metallicity (Fig. 2, inset). Note, however, that $\sigma_1(\omega)$ for the a axis remains finite at the lowest temperatures and frequencies reached, i.e., the energy gap is not fully developed. Thus we conclude that along the a and c axes, CeRu_4Sn_6 behaves predominantly insulator- and metal-like, respectively.

The temperature evolution of the integrated spectral weight $N_{\text{eff}}(\omega)$ for the a axis [Fig. 3(a)] suggests that the pseudogap is due to strong correlations as opposed to band effects: The spectral weight lost at low temperatures and energies due to the pseudogap formation is still not fully recovered at 0.6 eV, as similarly seen in other Kondo insulators.^{37,38} Interestingly, this effect, though smaller, can also be discerned for the c axis [Fig. 3(b)]. This indicates that a Kondo insulating gap exists also there.

The only other noncubic Kondo insulator for which $\sigma_1(\omega)$ results along the different crystallographic directions are

available is $\text{CeFe}_2\text{Al}_{10}$.³³ Here a Drude-like feature appears for all three crystallographic directions. The pronounced anisotropies observed in that system at higher temperatures and energies were attributed to an anisotropic Kondo temperature, in contrast to our findings (see below).

Can the salient features of CeRu_4Sn_6 be theoretically understood, and if so on which level of approximation? To answer this question, we performed, in a first step, LDA band-structure calculations [Fig. 4(a)]. They yield a direct (but no indirect) band gap of about 0.1 eV, separating Ru 4d and Sn 5p states below the Fermi level from Ce 4f states above it. The corresponding calculated $\sigma_1(\omega)$ is in strong disagreement with experiment [Fig. 4(b)]. In LDA + U, the 4f states are split by the Coulomb repulsion U so that one electron is transferred from the Ru 4d and Sn 5p to the Ce 4f orbital below the LDA + U Fermi level. Hence, part of the Ru and Sn states are now above the Fermi level [Fig. 4(c)] and CeRu_4Sn_6 is predicted to be metallic in all directions [Fig. 4(d)], again in contrast to experiment.

In a third step, LDA + DMFT calculations were performed at different temperatures. At high temperatures (~ 1000 K), the spectrum is similar to that of LDA + U (not shown). Upon reducing the temperature, we note the emergence of a Kondo resonance [red f -electron peak at the Fermi level in Figs. 5(a) and 5(c)]. This has dramatic consequences for $\sigma_1(\omega)$, which now shows good agreement with experiment [Fig. 5(b)]. Since the lowest experimental temperatures are not accessible in our theoretical approach, we mimic them by switching off the imaginary part of the self-energy [Fig. 5(c)]. This turns out to further enhance the anisotropy. In particular, below 0.1 eV, $\sigma_1(\omega)$ decreases sizably toward the lowest frequencies for the a axis while it levels out for the c axis [Fig. 5(d)], thus correctly reproducing the experimental trends.

The k -resolved LDA + DMFT spectrum reveals the origin of the anisotropy. At 290 K, the Ce 4f states are strongly broadened [smearing of bands around the Fermi level, Fig. 5(e)], which indicates the vicinity of the Kondo temperature where the scattering rate is high. At low temperatures, mimicked as above, the picture becomes clearer [Fig. 5(f)]: In large parts of

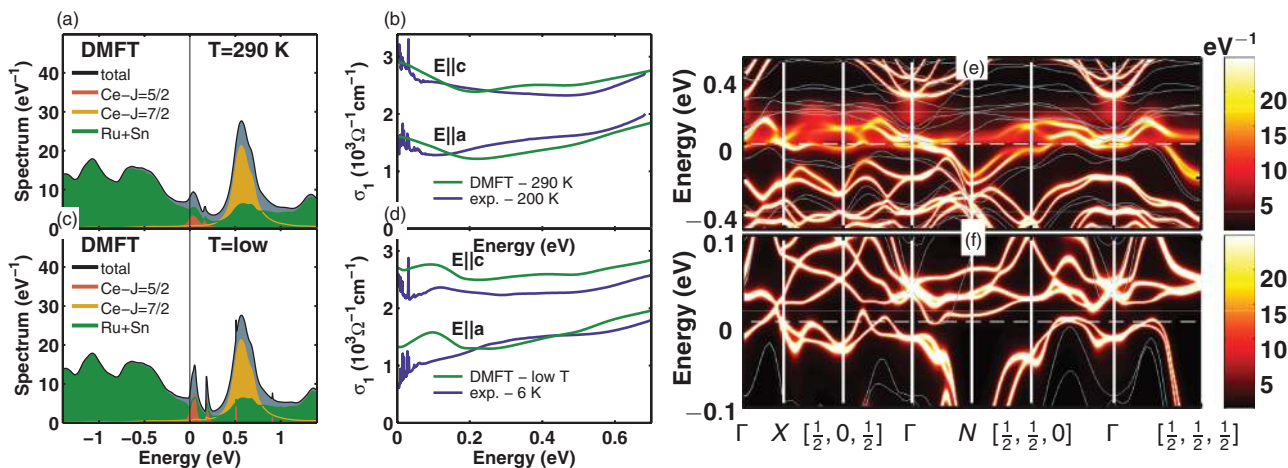


FIG. 5. (Color online) LDA + DMFT results: DOS at 290 K (a) and in the low-temperature limit (c), and the corresponding optical conductivities [(b,d) c -axis conductivities shifted by $+10^3 \Omega^{-1} \text{cm}^{-1}$ for clarity] and k -resolved spectra [(e,f) LDA band structure displayed as thin lines], showing a band crossing at the Fermi level for $\Gamma \rightarrow X$ (c axis) and a gap in the a - a plane.

the Brillouin zone, there is a direct gap reminiscent of a Kondo insulator, particularly within the tetragonal a - a plane; see, e.g., $\Gamma \rightarrow (\frac{1}{2}, \frac{1}{2}, 0)$. In contrast, in the c direction ($\Gamma \rightarrow X$) there is no such gap and the system is expected to show characteristics of a heavy fermion metal. Thus, the direct gap within the Kondo resonance varies between 0 and roughly 50 meV, depending on k [Fig. 5(f)]. Evidently, this complex behavior cannot be fitted by a single (or two) gap value. This explains the failure of such a fit in Fig. 1, resulting in a strongly temperature-dependent (fitted) gap value.

By its very nature the gap is a low-energy feature. It is a hybridization gap of size $\sqrt{|V(k)|^2 Z}$ (Ref. 41) within the already narrow Kondo resonance. Here, Z is the quasiparticle weight, which is proportional to the Kondo temperature T_K or the total width of the central (gapped) quasiparticle peak, and $V(k)$ is the k -dependent noninteracting LDA hybridization between f and conduction electrons. While T_K is isotropic, $V(k)$ is anisotropic and responsible for the k dependence of the gap, and for its vanishing along the c direction. Because of its low-energy scale, the anisotropy of the gap can only affect the optical conductivity at correspondingly low frequencies ($\lesssim 50$ meV). Indeed, Fig. 2 (inset) shows large anisotropies at such low energies.

In summary, we have investigated single-crystalline CeRu_4Sn_6 by optical reflectivity measurements and

LDA + DMFT calculations. The characteristic feature of an anisotropic Kondo insulator, its narrow anisotropic gap, can only be revealed at the lowest energies and temperatures. Experimentally, we observe a clear-cut anisotropy of the optical conductivity at such low energies: there are metal-like features along one direction but semiconductor-like features elsewhere. This can be traced back to the peculiar k dependence of the correlated LDA + DMFT bands. The weak metallicity of CeRu_4Sn_6 is thus clearly a bulk effect and not due to topologically protected metallic surface states.³⁹ It will be most enlightening to see whether magnetic Ising anisotropy goes along with this peculiar quasiparticle anisotropy and whether any relation to “hastatic order” in URu_2Si_2 (Ref. 40) can be established.

We thank M. Baenitz, M. Brando, A. Tóth, and A. Pimenov for fruitful discussions, A. Irizawa for sharing beam time at UVSOR, and K. Imura for technical assistance. V.G. benefited from financial support from the Alexander von Humboldt Foundation, P.W. and K.H. from the Austrian Science Fund (FWF-SFB ViCoM F41), H.W., A.P., and S.P. from the FWF (project I623-N16) and the European Research Council (ERC advanced grant 227378), and A.M.S from the DFG (OE 511/1-1) and the Science Faculty of UJ. Calculations were done on the Vienna Scientific Cluster.

-
- ¹H. Ding, T. Yokoya, J. C. Campuzano, T. Takahashi, M. Randeria, M. R. Norman, T. Mochiku, K. Kadowaki, and J. Giapintzakis, *Nature (London)* **382**, 6586 (1996).
- ²C. de la Cruz, Q. Huang, J. W. Lynn, J. Li, W. Ratcliff, J. L. Zarestky, H. A. Mook, G. F. Chen, J. L. Luo, N. L. Wang, and P. Dai, *Nature (London)* **453**, 899 (2008).
- ³O. Stockert, E. Faulhaber, G. Zwirgagl, N. Stüßer, H. S. Jeevan, M. Deppe, R. Borth, R. Küchler, M. Loewenhaupt, C. Geibel, and F. Steglich, *Phys. Rev. Lett.* **92**, 136401 (2004).
- ⁴A. R. Schmidt, M. H. Hamidian, P. Wahl, F. Meier, A. V. Balatsky, J. D. Garrett, T. J. Williams, G. M. Luke, and J. C. Davis, *Nature (London)* **465**, 570 (2010).
- ⁵P. Coleman, in *Handbook of Magnetism and Advanced Magnetic Materials*, edited by H. Kronmüller and S. Parkin (Wiley, West Sussex, UK, 2007), pp. 95–148.
- ⁶J. Levallois, F. Lévy-Bertrand, M. K. Tran, D. Stricker, J. A. Mydosh, Y.-K. Huang, and D. van der Marel, *Phys. Rev. B* **84**, 184420 (2011).
- ⁷W. K. Park, P. H. Tobash, F. Ronning, E. D. Bauer, J. L. Sarrao, J. D. Thompson, and L. H. Greene, *Phys. Rev. Lett.* **108**, 246403 (2012).
- ⁸F. F. Assaad, *Phys. Rev. Lett.* **83**, 796 (1999).
- ⁹J. Otsuki, H. Kusunose, and Y. Kuramoto, *Phys. Rev. Lett.* **102**, 017202 (2009).
- ¹⁰H. v. Löhneysen, A. Rosch, M. Vojta, and P. Wölfle, *Rev. Mod. Phys.* **79**, 1015 (2007).
- ¹¹G. R. Stewart, *Rev. Mod. Phys.* **56**, 755 (1984).
- ¹²T. Takabatake, F. Teshima, H. Fujii, S. Nishigori, T. Suzuki, T. Fujita, Y. Yamaguchi, J. Sakurai, and D. Jaccard, *Phys. Rev. B* **41**, 9607 (1990).
- ¹³M. Kyogaku, Y. Kitaoka, H. Nakamura, K. Asayama, T. Takabatake, F. Teshima, and H. Fujii, *J. Phys. Soc. Jpn.* **59**, 1728 (1990).
- ¹⁴H. Ikeda and K. Miyake, *J. Phys. Soc. Jpn.* **65**, 1769 (1996).
- ¹⁵J. Moreno and P. Coleman, *Phys. Rev. Lett.* **84**, 342 (2000).
- ¹⁶T. Yamada and Y. Ōno, *Phys. Rev. B* **85**, 165114 (2012).
- ¹⁷T. Takabatake, G. Nakamoto, T. Yoshino, H. Fujii, K. Izawa, S. Nishigori, H. Goshima, T. Suzuki, T. Fujita, K. Maezawa, T. Hiraoka, Y. Okayama, I. Oguro, A. A. Menovsky, A. B. K. Neumaier, and K. Andres, *Physica B* **223–224**, 413 (1996).
- ¹⁸P. Schlottmann, *Phys. Rev. B* **46**, 998 (1992).
- ¹⁹G. Venturini, B. Chafik El Idrissi, J. F. Maréché, and B. Malaman, *Mater. Res. Bull.* **25**, 1541 (1990).
- ²⁰I. Das and E. V. Sampathkumaran, *Phys. Rev. B* **46**, 4250 (1992).
- ²¹S. Paschen, H. Winkler, T. Nezu, M. Kriegisch, G. Hilscher, J. Custers, A. Prokofiev, and A. Strydom, *J. Phys.: Conf. Ser.* **200**, 012156 (2010).
- ²²B. P. Gorshunov, A. A. Volkov, A. S. Prokhorov, I. E. Spektor, J. Akimitsu, M. Dressel, G. Nieuwenhuys, S. Tomic, and S. Uchida, *Quantum Electron.* **37**, 916 (2007).
- ²³G. Kotliar, S. Y. Savrasov, K. Haule, V. S. Oudovenko, O. Parcollet, and C. A. Marianetti, *Rev. Mod. Phys.* **78**, 865 (2006).
- ²⁴K. Held, *Adv. Phys.* **56**, 829 (2007).
- ²⁵P. Blaha, K. Schwarz, P. Sorantin, and S. B. Trickey, *Comput. Phys. Commun.* **59**, 399 (1990).
- ²⁶J. Kunes, R. Arita, P. Wissgott, A. Toschi, H. Ikeda, and K. Held, *Comput. Phys. Commun.* **181**, 1888 (2010).
- ²⁷A. A. Mostofi, J. R. Yates, Y.-S. Lee, I. Souza, D. Vanderbilt, and N. Marzari, *Comput. Phys. Commun.* **178**, 685 (2008).
- ²⁸A. K. McMahan, K. Held, and R. T. Scalettar, *Phys. Rev. B* **67**, 075108 (2003).

- ²⁹J. E. Hirsch and R. M. Fye, *Phys. Rev. Lett.* **56**, 2521 (1986).
- ³⁰P. Wissgott, J. Kunes, A. Toschi, and K. Held, *Phys. Rev. B* **85**, 205133 (2012); P. Wissgott, E. Assmann, J. Kunes, A. Toschi, P. Blaha, and K. Held (unpublished) without a fixed phase of the Wien2K eigenfunctions.
- ³¹K.-i. Nakamura, Y. Kitaoka, K. Asayama, T. Takabatake, G. Nakamoto, H. Tanaka, and H. Fujii, *Phys. Rev. B* **53**, 6385 (1996).
- ³²V. H. Tran, S. Paschen, A. Rabis, N. Senthilkumaran, M. Baenitz, F. Steglich, P. de V. du Plessis, and A. M. Strydom, *Phys. Rev. B* **67**, 075111 (2003).
- ³³S. Kimura, Y. Muro, and T. Takabatake, *J. Phys. Soc. Jpn.* **80**, 033702 (2011).
- ³⁴E. M. Brüning, M. Brando, M. Baenitz, A. Bentien, A. M. Strydom, R. E. Walstedt, and F. Steglich, *Phys. Rev. B* **82**, 125115 (2010).
- ³⁵A. B. Kuzmenko, *Rev. Sci. Instrum.* **76**, 083108 (2005).
- ³⁶In the THz frequency range, $R(\omega)$ is very close to unity where small uncertainties in R can cause large errors in σ_1 . Therefore, $\sigma_1(\omega)$ was obtained by a weighted average over finite frequency ranges.
- ³⁷B. Bucher, Z. Schlesinger, P. C. Canfield, and Z. Fisk, *Phys. Rev. Lett.* **72**, 522 (1994).
- ³⁸Z. Schlesinger, Z. Fisk, H.-T. Zhang, M. B. Maple, J. F. DiTusa, and G. Aeppli, *Phys. Rev. Lett.* **71**, 1748 (1993).
- ³⁹M. Dzero, K. Sun, V. Galitski, and P. Coleman, *Phys. Rev. Lett.* **104**, 106408 (2010).
- ⁴⁰P. Chandra, P. Coleman, and R. Flint, *Nature (London)* **493**, 621 (2013).
- ⁴¹For a similar relation for a constant, i.e., k -independent $V(k)$, see A. C. Hewson, *The Kondo Problem to Heavy Fermions* (Cambridge University Press, Cambridge, 1993), Chap. 10.4.